

Magmatic Na-rich phlogopite in a suite of gabbroic crustal xenoliths from Volcán San Pedro, Chilean Andes: Evidence for a solvus relation between phlogopite and aspidolite

FIDEL COSTA,^{1,*} MICHAEL A. DUNGAN,¹ AND BRAD S. SINGER²

¹Section des Sciences de la Terre, Université de Genève, 13 Rue des Maraîchers, 1211 Genève, Switzerland.

²Department of Geology and Geophysics, University of Wisconsin-Madison, 1215 W. Dayton Street, Madison, Wisconsin 53706, U.S.A.

ABSTRACT

Magmatic Na-rich phlogopite (1–5 wt% Na₂O) is present as a late-crystallizing mineral in two groups of texturally and mineralogically distinct gabbroic xenoliths at Volcán San Pedro (36°S, Chile), an Andean arc volcano. Phlogopites are characterized by high 100-Mg/(Mg + Fe) (up to 83) and high Cr₂O₃ contents (up to 0.4 wt%), and they are always found surrounding variably resorbed olivine, pyroxenes, Cr-spinel, and in some cases, plagioclase. We interpret these micas as the result of open-system processes involving infiltration of water-rich evolved melts [with high Na/(Na + K)] and reaction with refractory minerals. The highest 100-Na/(Na + K) (~70) and Na₂O concentrations (~5 wt%) in phlogopite appear to require reaction with liquids of unrealistically high Na/(Na + K) if no other factor is considered. This, together with the observation that phlogopites consist of alternating Na-rich and Na-poor cleavage-parallel bands, can be best interpreted by the presence of a solvus between the aspidolite (Na) and phlogopite (K) end-members. The high proportions (up to 15 vol%) of Na-rich phlogopite in two different groups of gabbroic xenoliths suggest that it might be a more common and abundant mineral than has been previously recognized, and that it may be used as an indicator of open-system processes.

INTRODUCTION

Magmatic Na-rich phlogopite (e.g., Na₂O > 1 wt%) is an unusual mineral. Up to now, it has been recognized almost exclusively as an accessory mineral occurring in minute mono- or polymineralic inclusions in chromites of mafic layered intrusions (see Table 1; Irvine 1975; Morette et al. 1984; Talkington et al. 1986; Lorand and Cottin 1987), and ophiolite complexes (Augé 1987; Peng et al. 1995; Arai et al. 1997; Schiano et al. 1997). The only occurrence of Na-rich phlogopite not included in chromite was reported by Price and Sinton (1978) in the granitoid-gabbro suite of the Longwoods Complex, New Zealand. Aspidolite (recently resurrected by the International Mineralogical Association, is synonymous with the end-member Na phlogopite; Rieder et al. 1998) is commonly found in association with phlogopite, olivine, pyroxene, albite, feldspathoids, and Na-rich amphibole, and has been interpreted as the result of mixing between primitive water-poor magmas and aqueous fluids, or as the product of reactions between anhydrous minerals (olivine, pyroxenes, and plagioclase) and aqueous fluids (e.g., Peng et al. 1995).

Two groups of crustal gabbroic xenoliths of the calc-alkaline Volcán San Pedro (36°S, Chilean Andes) contain up to 15 vol% of Na-rich phlogopite (1–5 wt% Na₂O). Typically, the phlogopite surrounds resorbed refractory minerals. We propose

that these phlogopites are the result of open-system processes involving migration of evolved water-rich melts and reaction with early crystallized refractory minerals (olivine, Cr-spinel, pyroxenes, and plagioclase). However, the highest Na₂O concentrations (up to 5 wt%) and 100-Na/(Na + K) (up to 70) in phlogopite, apparently require, in addition, a solvus between the aspidolite and phlogopite end-members, analogous to the solvus reported for the Na (paragonite) and K (muscovite) white micas (e.g., Guidotti et al. 1994).

GEOLOGICAL SETTING

Holocene Volcán San Pedro is the youngest and most prominent volcanic edifice (3621 m) of the Quaternary Tatara-San Pedro Complex (~55 km²; TSPC), which is located on the volcanic front of the Southern Volcanic Zone of the Andes, at 36° S, 71°51' W (Singer et al. 1997). The TSPC comprises roughly 1 m.y. of volcanic activity, consisting mainly of lavas ranging from basalt to rhyolite that define medium- to high-K calc-alkaline trends (see Fig. 6 of Singer et al. 1997). The magmatic activity at Volcán San Pedro is divided into a cone-building phase comprising andesitic and dacitic lavas, and a younger phase that post-dates the sector collapse of the eastern flank of the volcano, which was accompanied by an explosive eruption that produced dacitic air-fall deposits (Singer and Dungan 1992). This was followed by the eruption of a sequence of lava flows that apparently records the downward tapping of a strongly zoned magma chamber. The eruptive sequence includes: (1) 0.2 km³ of biotite-hornblende dacite containing abundant gabbroic xenoliths (up to 45 cm in diameter) and

* Present Address: ISTO, 1A rue de la Ferrollerie 45071 Orleans cedex 2, France. E-mail: costaf@cnr-orleans.fr

TABLE 1. Occurrences of magmatic Na-rich phlogopite and aspidolite

Reference	Magmatic system	Rock type	Textural observations	wt% Na ₂ O in phlogopite
Irvine (1975)	Muskox intrusion	chromitite	inclusion in Cr-spinel	not reported
Price and Sinton (1978)	Longwoods Complex, New Zealand	peridotite	poikilitic surrounding Pl and Ol	<1–1.9
Morette et al. (1984)	Critical Zone of the Bushveld complex	chromitite	inclusion in Cr-spinel	6.4
Talkington et al. (1986)	J-M reef, Stillwater complex	chromitite	inclusion in Cr-spinel	<1–7.1
Augé (1987)	Oman ophiolite	chromitite	included in Cr-Spinel	1.2–6.4
Lorand and Cottin (1987)	Laouni intrusion (Algeria)	olivine-gabbro	inclusion in Cr-spinel	<1–7.2
Peng et al. (1995)	Hongguleleng ophiolite (China)	plagioclase dunite and chromitite	inclusion in Cr-spinel	<1–6.3
Arai et al. (1997)	MOR ultramafic and mafic plutonic rocks	gabbros and troctolites	inclusion in Cr-spinel	<1–5.5
Schiano et al. (1997)	Oman ophiolite	chromitite	inclusion in Cr-spinel	3.2–6.8
This work	Calc-alkaline Volcán San Pedro. Xenoliths	olivine-hornblende norites	poikilitic. Surrounding resorbed Ol and Cr-spinel	1–3.5
This work	Calc-alkaline Volcán San Pedro. Xenoliths	Hornblende norites	poikilitic. Surrounding resorbed Ol, Opx, Cr-spinel, and Pl	1–5
This work	Calc-alkaline Volcán San Pedro. Xenoliths	Clinopyroxene leuconorites	poikilitic and in microfractures	1–2.1

Note: Ol is olivine, Opx is orthopyroxene, and Pl is plagioclase.

quenched mafic inclusions; (2) 0.5 km³ of two-pyroxene dacite with abundant quenched mafic inclusions; and (3) 0.1 km³ of two-pyroxene andesite with rare quenched mafic inclusions. The last volcanic activity consisted of 0.2 km³ of basaltic andesitic magma (55–57 wt% SiO₂) that rebuilt the summit cone. The observation that the xenoliths are present exclusively in the first lava following sector collapse and the ensuing explosive eruption suggests that they are fragments of the conduits or upper parts of the margin of the San Pedro magma chamber that were shattered and incorporated during the eruption (in a similar fashion to the May 18, 1980 Mount St. Helens eruption; Heliker 1995).

TEXTURES OF THE GABBROIC XENOLITHS

We have divided the xenoliths into two main groups (Costa et al. in prep.). GROUP I consists of olivine-hornblende norites and melanorites (classification following Streckeisen 1976; Le Maitre 1989) that contain interstitial glass bounded by euhedral crystal faces, suggesting that GROUP I xenoliths are potentially co-magmatic with the Holocene San Pedro magmas. GROUP II xenoliths display subsolidus textures (e.g., exsolution lamellae in pyroxenes) and have been further subdivided into GROUP IICL, which are mainly clinopyroxene leuconorites, and GROUP IIHN which are hornblende norites. ⁴⁰Ar/³⁹Ar analyses suggest that GROUP II xenoliths are more than 1 Ma old (Costa et al. in prep), and thus they are fragments of the pre-Quaternary plutonic basement of the volcano.

GROUP I xenoliths: Olivine-hornblende norites

The samples consist of Cr-spinel, olivine, minor clinopyroxene, orthopyroxene, hornblende, plagioclase, and phlogopite forming a medium-grained (1–5 mm) crystal network with vesiculated SiO₂-rich (67–72 wt%) glass filling the interstices (0.5–13 vol%). Glass is bounded by euhedral crystal faces suggesting that it is residual from crystallization and not due to partial melting. Phlogopite makes up to 8 vol% and is euhedral to subhedral. Euhedral phlogopite occurs in the interstitial glass attesting to its magmatic origin and indicating that it was among the last minerals to crystallize (Fig. 1a). In most cases the phlogopite surrounds and encloses resorbed olivine and Cr-spinel (Fig. 1a), suggesting that a reaction occurred between these minerals and an evolved water-rich liquid.

GROUP II xenoliths: Clinopyroxene leuconorites and Hornblende norites with subsolidus textures

Clinopyroxene leuconorites (GROUP IICL) display seriate, mosaic textures with abundant plagioclase and orthopyroxene, and minor olivine, clinopyroxene, hornblende, phlogopite, Fe-Ti oxides, and Cr-spinel. Phlogopite (up to 15 vol%) occurs as small (<1 mm) anhedral crystals surrounding resorbed plagioclase, orthopyroxene, and Fe-Ti oxides (Fig. 1b). Phlogopite also fills discontinuous microfractures (<0.5 mm in width) together with hornblende, orthopyroxene, and Fe-Ti oxides (Fig. 1c).

Hornblende norites (GROUP IIHN) consist of large anhedral oikocrysts of hornblende (>1 cm across) that enclose resorbed,

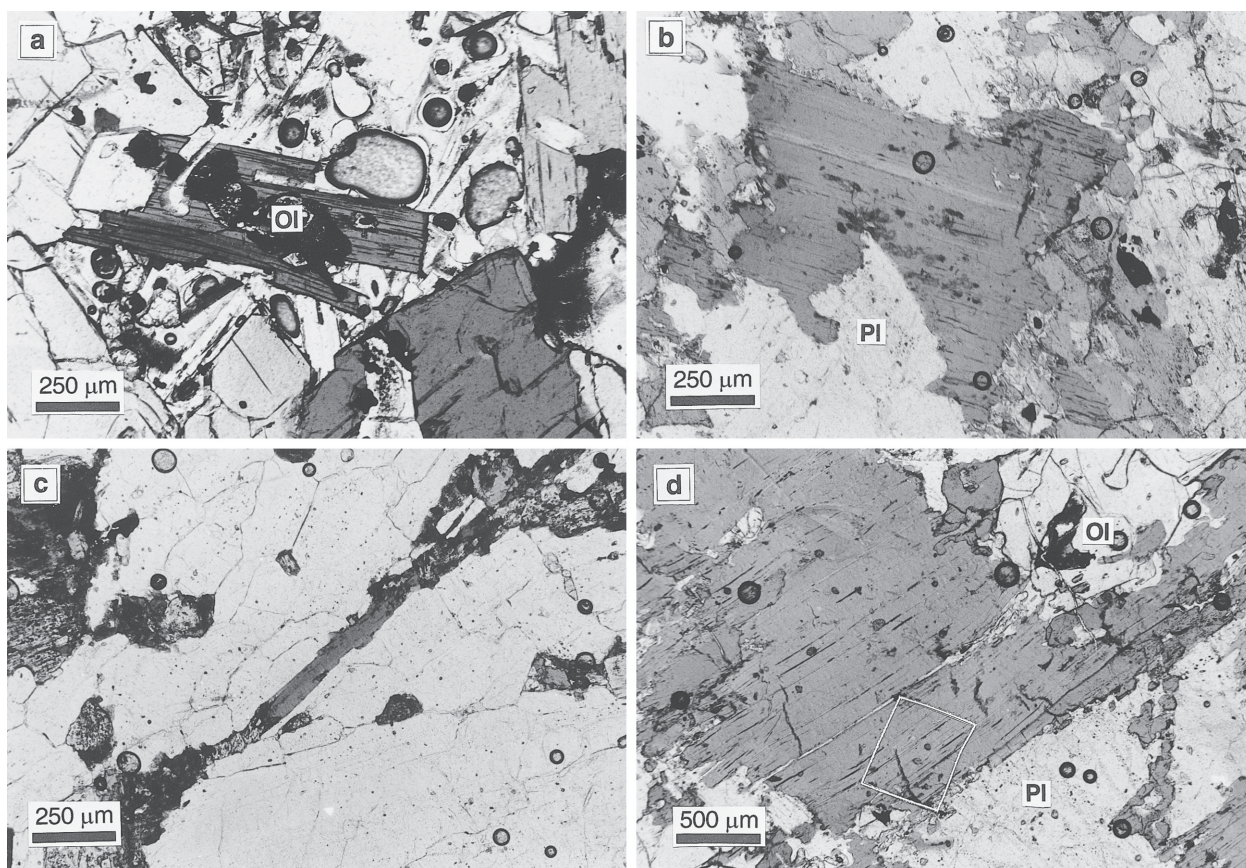


FIGURE 1. (a) GROUP I. Olivine-hornblende norite. Na-rich phlogopite surrounding resorbed olivine (Ol). Note euhedral margins of the mica in contact with vesicular interstitial glass. (b) GROUP II. Clinopyroxene leuconorite. Na-rich phlogopite surrounding corroded plagioclase (Pl). (c) GROUP II. Clinopyroxene leuconorite. Microfracture filled with phlogopite. (d) GROUP II. Hornblende norite. Na-rich phlogopite crystal with up to 5 wt% Na₂O; note resorbed plagioclase and olivine (Ol) in the vicinity. White square (empty) is the area of X-ray map shown in Figure 3.

anhedral olivine, Cr-spinel, clinopyroxene, orthopyroxene, and plagioclase. Phlogopite makes up to 4 vol% and is commonly subhedral to anhedral. It occurs inside hornblende crystals, surrounding resorbed olivine, Cr-spinel, orthopyroxene. In contrast to the GROUP I xenoliths, phlogopite also surrounds resorbed plagioclase (Fig. 1d).

PHLOGOPITE COMPOSITIONS

Electron microprobe analyses of phlogopite and of biotite from the host dacite lava were performed with a Cameca SX-50 instrument (University of Lausanne). Structural formulae were determined using 22 O atoms. The distinction between phlogopite and biotite follows Deer et al. (1962), in which phlogopite has $Mg/Fe_T > 2$ (based on cations per formula unit), where Fe_T is total Fe. Analytical details of the electron microprobe analyses are reported in Appendix 1.

GROUP I xenoliths: Olivine-hornblende norites

Phlogopites have Mg-numbers [= $100 \cdot Mg / (Mg + Fe_T)$ in mols] ranging from 82 to 77, and Cr₂O₃ concentrations from <0.05 to 0.43 wt%. The Na₂O contents are between 1.5 and 3.5 wt%, and Na-numbers [= $100 \cdot Na / (Na + K)$ in mols] that range

between 21 and 47 (Fig. 2). The occupancy of the A-site ranges from 1.9 to 2.1 (Table 2), which distinguishes these phlogopites from the interlayer-deficient mica wonesite (Spear et al. 1981). We interpret the high Cr₂O₃ contents and Mg-numbers of the phlogopites as due to reaction between olivine + Cr-spinel and an evolved water-bearing melt. The major element composition (e.g., MgO) of the phlogopites is comparable among different crystals, but minor elements (particularly Cr and Ba) are highly variable (Fig. 2), which probably reflects different melt/crystal reaction proportions. Volfinger and Robert (1980) and Volfinger et al. (1985) suggested a crystal-chemical control for the incorporation of Na in mica, particularly high Mg/Fe_T enhances substitution of Na for K. The importance of this factor is supported by the broad positive correlation between the Mg- and Na-numbers of the San Pedro phlogopites (Fig. 2).

GROUP II CL xenoliths: Clinopyroxene leuconorites

Poikilitic phlogopites have Mg-numbers that range from 81–70 and Cr₂O₃ contents are typically <0.2 wt%. Their Na₂O contents (1.1–2.1 wt%) and Na-numbers (15–28) are lower than those of phlogopites from GROUP I xenoliths (Fig. 2). Phlo-

gopites filling microfractures have lower Mg-numbers (76–70), lower Cr₂O₃ (<0.15 wt%) and Na₂O (0.7–1.3 wt%) contents, and lower Na-numbers (11–20) than poikilitic phlogopites (Table 2), and approach the compositions of the biotites found in the dacite lava. We propose that phlogopites filling microfractures crystallized from evolved, water-rich liquids comparable to the host dacite, and that the higher Mg-number and Cr₂O₃ contents of the poikilitic phlogopites are the result of reactions between mafic minerals (e.g., olivine, Cr-spinel, and pyroxenes) and evolved melts that migrated through the microfractures.

GROUP IIHN xenoliths: Hornblende norites

Phlogopites have Mg-numbers ranging from 84–77 and Cr₂O₃ contents up to 0.2 wt%. Most phlogopites have Na₂O contents between 1 and 2.5 wt%, except for one poikilitic crystal (3 mm across; Fig. 1d) that has up to 5 wt% Na₂O, and Na-numbers up to 68 (Fig. 2). An X-ray map of this phlogopite crystal (Fig. 3) shows that the Na concentration is not homogeneous. The crystal consists of alternating K-rich and Na-rich bands (<50 μm wide) parallel to the (001) cleavage direction. An electron microprobe traverse across the Na-rich zone of this

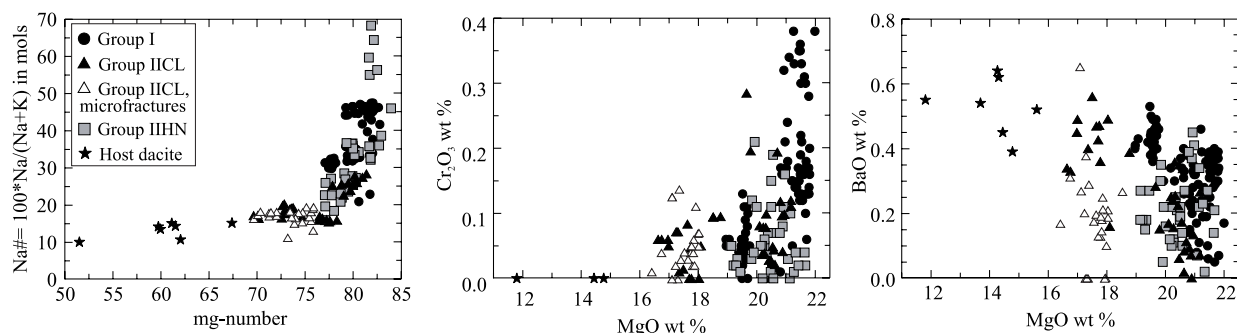


FIGURE 2. Variation diagrams showing phlogopite compositions from the xenoliths and of the biotites from the host dacite lava.

TABLE 2. Representative compositions of phlogopites from the xenoliths and biotites of the host dacite lava

wt%	Group I xenoliths Olivine-Hornblende norites					Group II CL. Clinopyroxene leuconorites					
	b-2-4	b-1-1	k-2-10	n-1-4	n-2-1	a-6-p	e-IV-1p	e-I-3p	a-1-v	w-10-v	w-6-v
SiO ₂	37.45	37.11	38.58	37.97	37.55	37.19	37.06	36.87	38.8	36.45	37.1
TiO ₂	2.19	2.58	1.10	0.63	0.75	4.77	2.63	0.73	3.42	5.22	5.11
Al ₂ O ₃	16.43	16.53	16.47	16.12	16.27	14.18	16.48	16.18	13.5	13.98	13.8
Cr ₂ O ₃	0.06	0.01	0.4	—	—	0.06	0.03	0.12	0.05	0.00	0.06
FeO*	9.90	10.01	9.04	9.35	9.20	12.94	8.37	9.23	13.4	10.81	10.8
MnO	0.07	0.05	0.10	0.00	0.01	0.13	0.08	0.09	0.12	0.02	0.09
MgO	19.50	19.46	21.20	21.14	20.81	16.63	20.46	21.17	17.8	17.29	17.9
CaO	0.01	0.01	0.07	0.00	0.07	0.03	0.03	0.04	0.04	0.15	0.11
Na ₂ O	2.30	2.22	3.11	2.34	2.29	1.18	2.07	1.92	1.25	1.08	1.21
K ₂ O	7.40	7.54	5.43	7.39	7.21	8.64	7.91	8.25	8.52	8.31	8.26
BaO	0.45	0.53	0.21	0.11	0.14	0.34	0.35	0.07	0.13	0.38	0.21
F	0.17	0.15	0.08	0.15	0.17	0.22	0.00	0.00	0.14	0.48	0.38
Cl	0.05	0.03	0.06	0.06	0.04	0.12	0.11	0.08	0.13	0.24	0.17
O=F	0.07	0.06	0.03	0.06	0.07	0.09	0.00	0.00	0.06	0.20	0.16
O=Cl	0.01	0.01	0.01	0.01	0.01	0.03	0.02	0.02	0.03	0.05	0.04
Sum	95.90	96.16	95.83	95.18	94.43	96.3	95.54	94.72	97.22	94.15	94.93
Formula proportions of cations based on 22 O Atoms											
Si	5.43	5.37	5.5	5.51	5.48	5.48	5.36	5.40	5.65	5.46	5.49
Al	2.80	2.82	2.77	2.75	2.80	2.46	2.81	2.79	2.31	2.47	2.41
Cr	0.01	0.00	0.05	—	—	0.01	0.00	0.01	0.01	0.00	0.01
Ti	0.24	0.28	0.12	0.07	0.08	0.53	0.29	0.08	0.37	0.59	0.57
Mg	4.21	4.20	4.51	4.57	4.53	3.66	4.41	4.63	3.86	3.86	3.93
Fe	1.20	1.21	1.08	1.13	1.12	1.60	1.01	1.13	1.63	1.35	1.33
Mn	0.01	0.01	0.01	0.00	0.00	0.02	0.01	0.02	0.00	0.01	0.01
Ca	0.00	0.00	0.01	0.00	0.01	0.01	0.00	0.01	0.01	0.02	0.02
Na	0.65	0.62	0.86	0.66	0.65	0.34	0.58	0.54	0.35	0.31	0.35
K	1.37	1.39	0.99	0.37	1.34	1.63	1.46	1.54	1.58	1.58	1.59
Ba	0.03	0.03	0.01	0.01	0.01	0.02	0.02	0.00	0.01	0.02	0.01
A-site	2.04	2.05	1.87	2.03	2.01	1.99	2.06	2.09	1.95	1.95	1.94
Mg-number	77.8	77.6	80.7	80.1	80.1	69.6	81.3	80.3	70.3	74.0	74.7
Na-number	32.1	30.9	46.5	32.5	32.6	17.2	28.4	26.1	18.2	16.5	18.2

Note: * = total iron as FeO. Mg-number = 100 · Mg/(Mg+Fe_T), in mols and Fe_T is total Fe. "p" indicates poikilitic crystal, "v" indicates crystal in microfractures, Na-number = 100 · Na/(Na+K) in mols. A-site = Ca + Na + K + Ba.

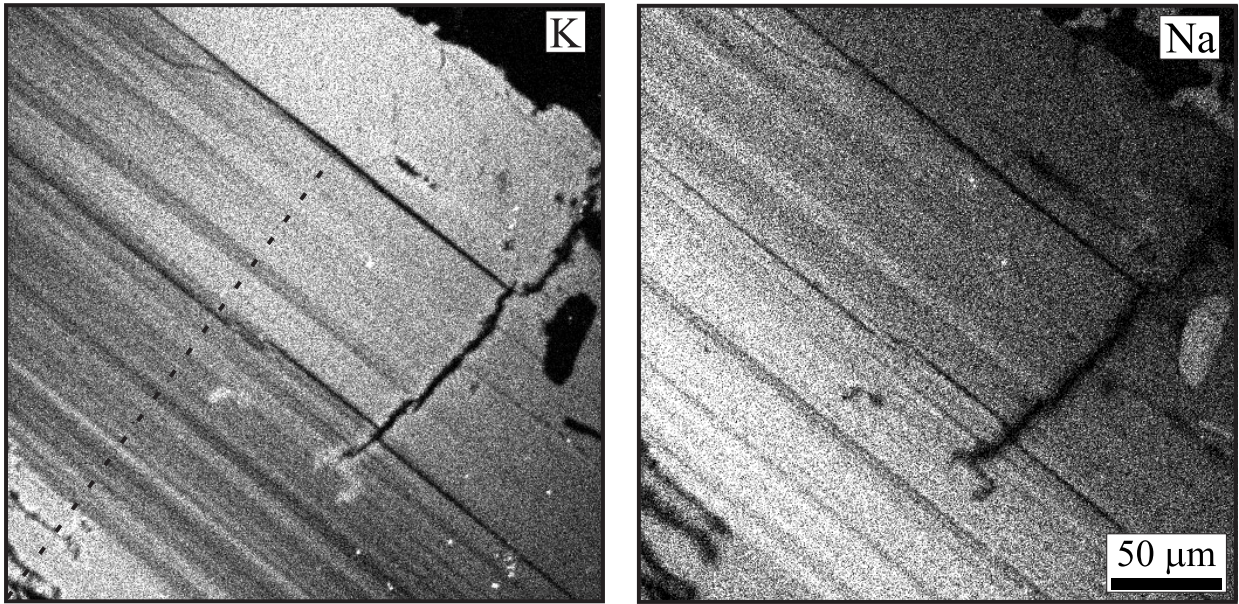


FIGURE 3. X-ray map of Na and K distribution of the phlogopite with up to 5 wt% Na₂O. Na and K are distributed as bands approximately parallel to the (001) cleavage (bright areas reflect high concentrations). The mapped area is marked in Figure 1d. The dashed line marks the position of the electron microprobe traverse shown in Figure 4.

TABLE 2. —Extended

Group II xenoliths					Dacite lava	
Group IIHN. Hornblende norites					bt-1r	bt-2c
v-III-8	v-III-10	v-III-11	v-I-3	z-ii-1		
38.62	39.16	38.70	38.8	38.18	36.97	34.70
1.94	2.09	2.06	1.44	2.32	4.23	4.54
17.32	17.73	17.97	17.1	16.41	13.87	13.54
0.08	0.10	0.11	0.03	0.21	0.00	0.00
8.35	8.37	8.41	8.4	8.94	17.38	19.83
0.06	0.06	0.10	0.07	0.03	0.18	0.30
20.89	21.15	20.92	21.1	19.93	14.44	11.80
0.03	0.08	0.08	0.01	0.01	0.00	0.00
4.08	4.89	4.32	2.56	1.96	0.96	0.66
5.06	3.45	4.43	7.02	7.91	8.81	8.97
0.37	0.34	0.45	0.07	0.22	0.45	0.55
0.13	0.08	0.10	0.11	0.19	0.00	0.00
0.06	0.05	0.05	0.09	0.12	0.00	0.00
0.05	0.03	0.04	0.05	0.08	0.00	0.00
0.01	0.01	0.01	0.02	0.03	0.00	0.00
96.92	97.51	97.65	96.78	96.32	97.3	94.9
5.43	5.43	5.39	5.49	5.49	5.48	5.51
2.87	2.90	2.95	2.85	2.77	2.43	2.49
0.01	0.01	0.01	0.00	0.02	0.00	0.00
0.21	0.22	0.22	0.15	0.25	0.47	0.53
4.38	4.37	4.34	4.44	4.26	3.21	2.74
0.98	0.97	0.98	0.99	1.07	2.16	2.58
0.01	0.01	0.01	0.01	0.00	0.02	0.04
0.01	0.01	0.01	0.00	0.00	0.00	0.00
1.11	1.31	1.17	0.70	0.55	0.28	0.20
1.56	0.91	0.61	0.79	1.26	1.45	1.67
0.02	0.02	0.03	0.00	0.01	0.03	0.03
2.05	1.96	1.99	1.97	2.01	1.98	2.02
81.7	81.8	81.6	81.7	79.9	59.7	51.5
55.1	68.3	59.7	35.7	27.4	14.2	10.1

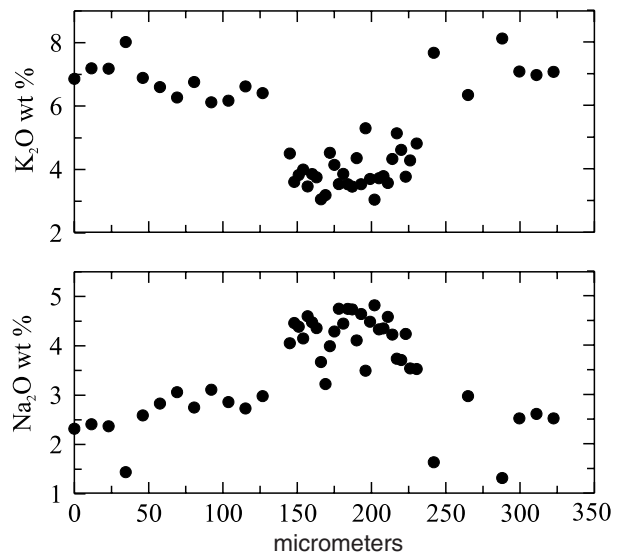


FIGURE 4. Electron microprobe traverse across a Na-rich zone of the phlogopite crystal shown in Figure 3. The Na-rich zone is complementary to K-poor zones. Within the Na-rich zone, variations of up to 2 wt% of Na₂O occur, suggesting that it consists of mixtures of aspidolite and phlogopite. Note that the spacing of the electron microprobe analyses in the Na-rich zone is 5 times smaller (2 μm) than for the rest of the traverse.

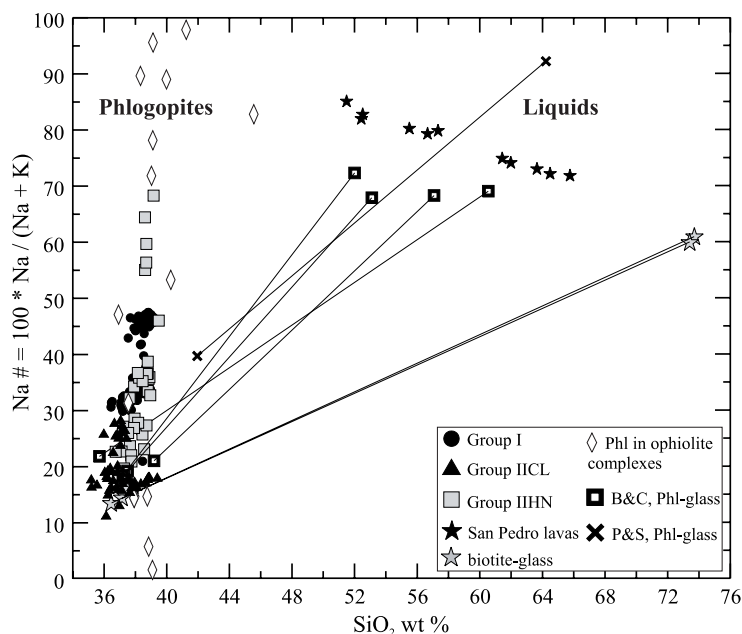


FIGURE 5. Phlogopite-coexisting liquid tie-lines from the unpublished experiments of Barclay and Carmichael (in prep.) and from Prouteau (1999). Also plotted are the tie lines between biotite and interstitial glass of the host dacite. The compositions of phlogopites and aspidolites from ophiolite complexes are from: Hongguleleng ophiolite (Peng et al. 1995); mid-oceanic ridge mafic and ultramafic rocks (Arai et al. 1997); Oman ophiolite (Schiano et al. 1997). Data from the Laouni intrusion (Lorand and Cottin 1987) are also included. See text for discussion.

phlogopite crystal (Fig. 4) shows that variations of up to 2 wt% Na_2O occur in less than 10 μm , suggesting that even the Na-rich zones are heterogeneous and probably consist of fine (<1–2 μm) intergrowths of aspidolite and phlogopite. Such abrupt changes in the concentrations of Na_2O and K_2O in phlogopite are difficult to explain by changes in the liquid composition alone, and they probably reflect the presence of a solvus.

DISCUSSION

The reaction textures and composition (e.g., high Cr_2O_3 and Mg-number) displayed by most phlogopites of the San Pedro gabbroic xenoliths suggest that they are the products of reactions between evolved water-rich liquids and olivine, pyroxenes, and Cr-spinel. Such reactions are unlikely to be the result of progressive closed-system crystallization, as experiments on medium-K, calc-alkaline water-rich liquids (e.g., Sisson and Grove 1993) have not yielded Na-rich phlogopite, or phlogopite even at crystallinities of up to 90% (Kawamoto 1996). Moreover, the microfractures filled with phlogopite in GROUP II xenoliths are evidence of open-system processes involving migration of evolved water-rich melts.

To explain the high Na-numbers of most phlogopites, we consider below: (1) the possibility that plagioclase was involved in the phlogopite-forming reactions; (2) the composition of the reacting liquids; and (3) the potential role of a solvus.

Is plagioclase responsible for the high Na-number of the phlogopite?

Textural relations of GROUP II xenoliths suggest that plagioclase could have participated in the phlogopite-forming reaction, and thus it could be responsible, at least in part, for the high Na-number of phlogopite. However, this interpretation cannot explain the high Na-number of phlogopites in GROUP I xenoliths, where textural relations indicate that plagioclase

was stable during phlogopite crystallization. The fact that Na is concentrated in bands instead of being distributed homogeneously in the phlogopite crystal with the highest Na_2O content (Fig. 3) also argues against consumption of plagioclase as the sole explanation for the high Na-number of the phlogopites.

Composition of the reacting liquids

The compositions of liquids from which the San Pedro phlogopites crystallized can be assessed by comparing their Na-numbers to those of phlogopites crystallized from experiments. Aside from experiments of Carman (1974) on K-free synthetic compositions and those of Liu (1989) on hydrothermal solutions, the only other experiments that have produced phlogopite with significant amounts of Na_2O (e.g., > 1 wt%) are the unpublished results of Barclay and Carmichael (in prep.) on a trachybasaltic composition, and those of Prouteau (1999) involving reaction between trondhjemitic liquids and forsteritic olivine. Figure 5 shows the tie-lines joining phlogopites and coexisting liquid compositions from experiments and those of biotite and interstitial glass of the host dacite lava. Phlogopites of the San Pedro xenoliths with Na-numbers up to ~30, which corresponds to ~2.5 wt% Na_2O , could have crystallized from liquid compositions similar to the dacites of Volcán San Pedro (Fig. 5), although we cannot rule out the possibility that such phlogopites consist of mixtures of aspidolite and phlogopite intergrowths. The rest of the phlogopites have Na-numbers (up to 68) that seem to require reaction with liquids of unrealistically high Na-numbers. Even the phlogopite that crystallized from a trondhjemitic liquid has an Na-number of only 40 (Fig. 5).

A solvus relation among phlogopite and aspidolite (Na phlogopite)

The extremely high Na-number (68) and Na_2O contents (5 wt%) of some phlogopites seem to be explained best by the

existence of a solvus between the aspidolite (Na) and phlogopite (K) end-members. Confirmation of this hypothesis would require finding discreet coexisting crystals from each side of the solvus. In the San Pedro xenoliths, the phlogopites with the highest Na contents are found in a single crystal and are intergrown with Na-poor phlogopite (Figs. 3 and 4), and thus it could be argued that they represent a metastable solvus. Supporting evidence for the existence of a stable solvus includes the unpublished hydrothermal ion-exchange experiments of Liu (1989), who found a miscibility gap between aspidolite and phlogopite at 2 kbar and 700 °C for compositions having Na-numbers that range from 40 to 70. In addition, the mode of occurrence and composition of micas present in chromite inclusions of ophiolite complexes also suggest the presence of a solvus. In many cases, aspidolite and phlogopite coexist as separate crystals inside a single chromite grain (e.g., Peng et al. 1995; Schiano et al. 1997) suggesting that the two micas co-crystallized from a single liquid. The proposed solvus between the aspidolite (Na) and phlogopite (K) end-members is probably analogous to that recognized for the Na (paragonite) and K (muscovite) white micas (e.g., Guidotti et al. 1994).

ACKNOWLEDGMENTS

We are grateful to J. Barclay, G. Prouteau, and B. Scaillet for making available to us their unpublished experimental data, and to J.-L. Robert for providing us with the unpublished thesis of Liu (1989). We thank B. Evans for the helpful suggestions concerning the possible importance of a solvus relationship in this system. We also thank J. Davidson, A. McBirney, and P. Ulmer for comments on an earlier version of the manuscript, and the reviews of C.V. Guidotti and J.-L. Robert, which helped us to clarify various aspects of the manuscript. Field work was supported by a grant from the Swiss Academy of Natural Sciences, and by research grants 20-42124-94 and 20-49730-96 of the Swiss National Fonds.

REFERENCES CITED

- Arai, S., Matsukage, K., Isobe, E., and Vysotskiy, S. (1997) Concentration of incompatible elements in oceanic mantle: Effect of melt/wall interaction in stagnant or failed melt conduits within peridotite. *Geochimica et Cosmochimica Acta*, 61, 671–675.
- Augé, T. (1987) Chromite deposits in the northern Oman ophiolite: mineralogical constraints. *Mineralium Deposita*, 22, 1–10.
- Carman, J.H. (1974) Synthetic sodium phlogopite and its two hydrates: stabilities, properties and mineralogical implications. *American Mineralogist*, 59, 261–273.
- Deer, W.A., Howie, R.A., and Zussman, J. (1962) *Rock forming minerals*. Vol.3. Sheet silicates, 270 p. Longman, London.
- Guidotti, C.V., Sassi, F.P., Blencoe, J.G., and Selverstone, J. (1994) The paragonite-muscovite solvus: I. P-T-X limits derived from the Na-K compositions of natural, quasibinary paragonite-muscovite pairs. *Geochimica et Cosmochimica Acta*, 58, 2269–2275.
- Heliker, C. (1995) Inclusions in Mount St. Helens dacite erupted from 1980 through 1983. *Journal of Volcanology and Geothermal Research*, 66, 115–135.
- Irvine, T.N. (1975) Crystallization sequences in the Muskox intrusion and other layered intrusions-II. Origin of chromitite layers and similar deposits of other magmatic ores. *Geochimica et Cosmochimica Acta*, 39, 991–1020.
- Kawamoto, T. (1996) Experimental constraints on differentiation and water abundance of calc-alkaline magmas. *Earth and Planetary Science Letters*, 144, 577–589.
- Le Maitre, R.W., Ed. (1989) *A classification of igneous rocks and glossary of terms*. Blackwell, Oxford, 193 pp.
- Liu, Xiang Feng (1989) Signification pétrogénétique des micas trioctédriques sodiques. Modélisation expérimentale dans le système Na₂O-K₂O-MgO-Al₂O₃-SiO₂-H₂O-(TiO₂-HF-D₂O). Thèse de Doctorat; Université d'Orléans, 87 p.
- Lorand, J.-P. and Cottin, J.-Y. (1987) Na-Ti-Zr-H₂O-rich mineral inclusions indicating postcumulus chrome-spinel dissolution and recrystallization in the West Laouni mafic intrusion, Algeria. *Contributions to Mineralogy and Petrology*, 97, 251–263.
- Morette, Y., Watkinson, D., Robert, J.-L., and Johan, Z. (1984) Rôle des fluides dans la précipitation des spinelles, chromite et magnétite, à partir de magmas du Bushveld. *Bulletin de Minéralogie, Supplément*, 107, 44.
- Peng, G., Lewis, J., Lipin, B., McGee, J., Bao, P., and Wang, X. (1995) Inclusions of phlogopite and phlogopite hydrates in chromite from the Hongguleleng ophiolite in Xinjiang, northwest China. *American Mineralogist*, 80, 1307–1316.
- Price, R.C. and Sinton, J.M. (1978) Geochemical variations in a suite of granitoids and gabbros from Southland, New Zealand. *Contributions to Mineralogy and Petrology*, 67, 267–278.
- Prouteau, G. (1999) Contribution des produits de fusion de la croûte océanique subductée au magmatisme d'arc: exemples du Sud-Est asiatique et approche expérimentale. Thèse Université de Bretagne Occidentale, 300 pp.
- Rieder, M., Cavazzini, G., D'yakonov, Y.S., Frank-Kamenetskii, V.A., Gottardi, G., Guggenheim, S., Koval, P.V., Müller, G., Neiva, A.M.R., Radoslovich, E.W., Robert, J.-L., Sassi, F.P., Takeda, H., Weiss, Z., and Wones, D.R. (1998) Nomenclature of the micas. *American Mineralogist*, 83, 1366.
- Schiano, P., Clocchiatti, R., Lorand, J.-P., Massare, D., Delouie, E., and Chaussidon, M. (1997) Primitive basaltic melts included in podiform chromites from the Oman Ophiolite. *Earth and Planetary Science Letters*, 146, 489–497.
- Singer, B.S. and Dungan, M.A. (1992) The origin of compositionally zoned Holocene magma at Volcán San Pedro, Chilean Andes. *EOS*, 73, 644.
- Singer, B.S., Thompson, R.A., Dungan, M.A., Feeley, T.C., Nelson, S.T., Pickens, J.C., Brown, L.L., Wulff, A.W., Davidson, J.P., and Metzger, J. (1997) Volcanism and erosion during the past 930 k.y. at the Tatara-San Pedro complex, Chilean Andes. *Geological Society of America Bulletin*, 109, 127–142.
- Sisson, T.W. and Grove, T.L. (1993) Experimental investigations of the role of H₂O in calc-alkaline differentiation and subduction zone magmatism. *Contributions to Mineralogy and Petrology*, 113, 143–166.
- Spear, F.S., Hazen, R.M., and Rumble, D. III (1981) Wonesite: a new rock-forming silicate from the Post Pond Volcanics, Vermont. *American Mineralogist*, 66, 100–105.
- Strecker, A. (1976) To each plutonic rock its proper name. *Earth and Science Reviews*, 12, 1–33.
- Talkington, R.W., Watkinson, D.H., Whittaker, P.J., and Jones, P.C. (1986) Platinum group element-bearing minerals and other solid inclusions in chromite of mafic and ultramafic complexes: chemical compositions and comparisons. In: B. Carter, M.K.R. Chowdhury, S. Jankovik, A.A. Marakushev, L. Morten, V.V. Onikhimovsky, G. Raade, G. Rocci, and S.S. Augustithis, Eds., *Metallurgy of basic and ultramafic rocks (regional presentations)*, 223–249. Theophrastus, Athens, Greece.
- Volfinger, M. and Robert, J.-L. (1980) Structural control of the distribution of trace elements between silicates and hydrothermal solutions. *Geochimica et Cosmochimica Acta*, 44, 1455–1461.
- Volfinger, M., Robert, J.-L., Vielzeuf, D., and Neiva, A.M.R. (1985) Structural control of the chlorine content of OH-bearing silicates (micas and amphiboles). *Geochimica et Cosmochimica Acta*, 49, 37–48.

MANUSCRIPT RECEIVED MARCH 1, 2000

MANUSCRIPT ACCEPTED SEPTEMBER 18, 2000

PAPER HANDLED BY WENDY BOHRSON

APPENDIX 1. ANALYTICAL TECHNIQUES

Electron microprobe analyses were performed with a SX-50 Cameca instrument at the University of Lausanne. Accelerating voltage was 15 kV, beam current 15 nA, and beam diameter 2 µm. Typical two sigma relative precisions (in %) are as follows: SiO₂ (0.9), TiO₂ (5–10), Al₂O₃ (1–1.5), Cr₂O₃ (12–40), FeO* (3), MnO (30 to below detection), MgO (1), CaO (30 to below detection), Na₂O (3–6), K₂O (2–2.5), BaO (25 to below detection), F (25 to below detection), Cl (30–50). X-ray mapping of Na and K was done by rastering the electron beam with an accelerating voltage of 15 kV and beam current of 30 nA. We used the following standards: diopside for Si; MnTiO₃ for Ti and Mn; bytownite for Al and Ca; Cr₂O₃ for Cr; andradite for Fe; F-phlogopite for Mg, K, and F; albite for Na; benitoite for Ba; and tugtupite for Cl.